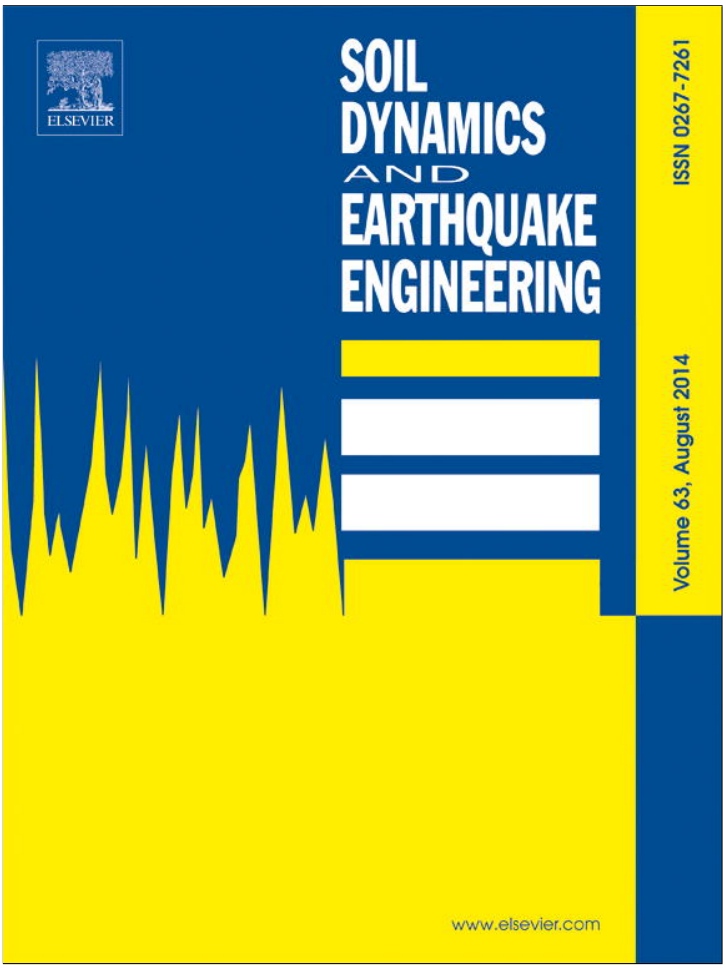

Soil Dynamics and Earthquake Engineering 63 (2014) 1–7

Contents lists available at ScienceDirect

Soil Dynamics and Earthquake Engineering

journal homepage: www.elsevier.com/locate/soildyn

Technical Note

Small-strain dynamic characterization of clayey soil from the Texcoco Lake, Mexico

Mario Flores-Guzmán [a], Efraín Ovando-Shelley [a,*], Celestino Valle-Molina [b]

[a] Instituto de Ingeniería, UNAM, Ciudad Universitaria, Coyoacán 04510, DF, Mexico City, Mexico
[b] Instituto Mexicano del Petróleo, Eje Central Lázaro Cádenas 152, Mexico City 07730, Mexico

ARTICLE INFO

Article history:
Received 29 July 2013
Received in revised form
7 March 2014
Accepted 11 March 2014
Available online 4 April 2014

Keywords:
Texcoco Lake clay
Shear wave velocities
Piezoelectric transducers
Bender elements
Resonant column
Seismic cone

ABSTRACT

The area occupied by the former Texcoco Lake was part of a system of lakes inside the Basin of Mexico. The subsoil there has been studied in the past but there is still a need for more and more thorough investigations into the dynamic properties of its highly compressible clays. This paper describes the results of an experimental laboratory research in which a triaxial cell fitted with bender elements was used to measure shear wave velocities (V_s) in clay specimens from the former Texcoco Lake. Soil specimens were subjected to isotropic loading–unloading cycles and values of V_s were determined during the saturation stage and after each stress increment or decrement. Our results show that irrespective of the testing method, shear waves velocities differ in no more than 7–15%.

1. Introduction

Researchers have carried out investigations into the basic engineering properties of Mexico City clays for more than 60 years. Still, there are many aspects of the behavior of the lacustrine Mexico City clays that require further research, especially those located in what used to be the former Texcoco Lake, located in the northern portion of the Mexico Valley. Characteristics of the soils in lake zone of Mexico City have been extensively studied by Marsal and Mazari [1], Carillo [2], Ovando et al. [3], among others. Field and lab investigations have been reported in a number of studies [4,5]. Specific studies into the dynamic properties of the former Texcoco Lake clays are fewer, like those collected by Mayoral et al. [6].

This note shows that piezoelectric transducers can be used efficiently and advantageously to study the dynamic properties of the lacustrine clays of the former Texcoco Lake.

2. Geotechnical conditions in the former Texcoco Lake

The larger part of the soil deposits in the former Lake Texcoco have never been subjected to external overburdens. Nonetheless, the zone has been subjected to the effects of deep well pumping

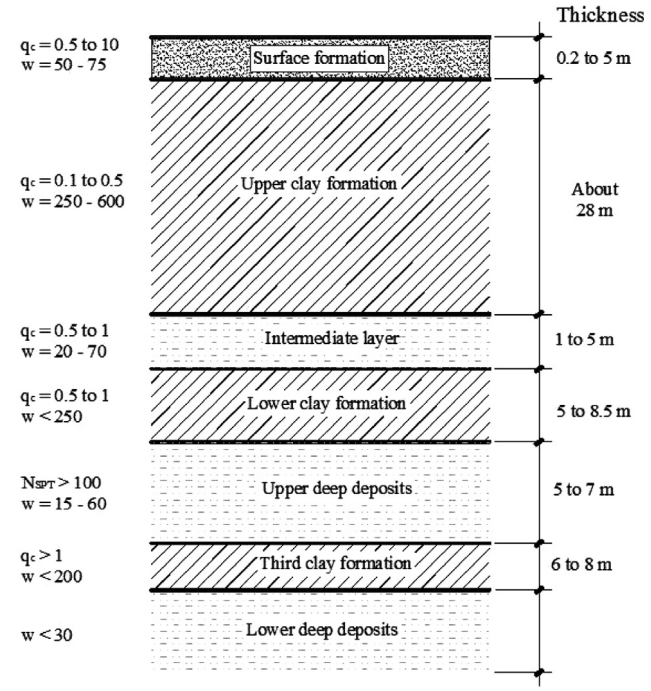

Fig. 1. Typical stratigraphic profile at the former Texcoco lake [4].

* Corresponding author. Tel.: +52 55 5623 3649.
E-mail addresses: mfloresg@iingen.unam.mx (M. Flores-Guzmán), eovs@pumas.ii.unam.mx (E. Ovando-Shelley), cvallem@imp.mx (C. Valle-Molina).

http://dx.doi.org/10.1016/j.soildyn.2014.03.005
0267-7261/

and, also, to very intense shallow pumping in the western portion, for the production of caustic soda. Local and regional pumping induced total settlements in the zone of more than 8 m over a 20 year period [7].

As seen in Fig. 1, the subsoil is constituted by three potent layers of lacustrine soft clay interspersed with layers and lenses of other harder more permeable materials. Thicknesses of the main strata and typical water contents are indicated in the figure, as well as illustrative cone penetration strengths values or blow counts from standard penetration tests.

The most compressible stratum is the upper clay formation in which water contents are extremely high, as shown in the figure. Thin lenses and layers of coarser alluvial soils are often found interspersed with these highly plastic clays. The uppermost materials are slightly preconsolidated due to solar drying. Even though other compressible strata can also be found at larger depths, the characterization of these clays is of paramount importance in foundation problems in the former Texcoco Lake. Also, seismic movements at the site are largely influenced by the dynamic response of these clays and that is why the samples used in the experimental research presented here were retrieved from these strata.

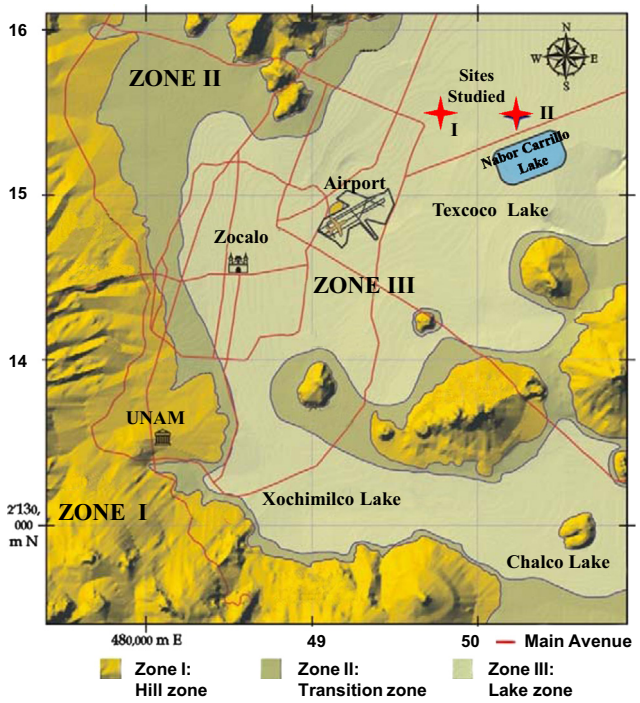

Fig. 2. Location of the study sites in the former Texcoco Lake.

3. Experimental techniques

Essentially, this experimental technique consists of propagating body waves and identifying the wave arrivals and travel times with the receiving transducer (direct-arrival-time technique).

Techniques and procedures for measuring shear wave velocities, V_s, have been discussed previously [8–10]. In this research, we used zirconate–titanate bender elements to measure shear wave velocities (V_s) propagating in soil specimens. Also, it was necessary to develop a data acquisition system to record and analyze the measured signals with the piezoelectric transducers.

A sinusoidal signal was used to excite the source-transducer, since it is simpler to determine wave arrival time in comparison with measurements performed using square signals [9]. The optimum frequency of excitation to identify the arrival time of the S-wave was 2 kHz.

A confining pressure and a back pressure were applied to the specimens to reach full saturation (maintaining an effective stress of 10 kPa). After the specimens were fully saturated (Skempton´s B parameter close to unity, [11]), consolidation under isotropic loading was started. Soil specimens were consolidated applying a maximum effective stress equal to twice the effective vertical pressure *in situ*. After the end of primary consolidation, the next increment of pressure was applied until reaching the branch of virgin consolidation line. V_s were measured for each increment of effective stress. The specimens were taken to failure under undrained conditions after reaching the maximum isotropic stress.

4. Laboratory results

The soil specimens we used in this research were retrieved from the upper clay formation at two sites in the former Texcoco Lake (Fig. 2). High quality samples were extracted with a thin-walled aluminum tube sampler designed specifically for the very soft soils found in and around Mexico City [12]. The initial index properties of the six specimens tested in this study are listed in Table 1 as well as sample retrieval depths, sample geometry and testing apparatuses used.

After saturation V_s were measured in specimens 1–4 under different isotropic effective stresses, along two cycles of loading and unloading and a final reloading stage. Seismic measurements were performed before each increment or decrement of effective stress. Specimens 1 and 3 were subjected to two loading and unloading cycles followed by a final reloading stage in the instrumented triaxial cell, as indicated in Tables 2 and 3. Specimens 2 and 4 were tested in a Drnevich type resonant column; we only applied one loading–unloading cycle (see Table 4). Specimens 5 and 6 were also consolidated isotropically in the triaxial cell, measuring V_s along the virgin compression curve.

Table 1
Initial properties of the specimens of Sites I and II from Texcoco Lake.

Site	Specimen no.	Diameter (cm)	Height (cm)	Depth (m)	Void ratio (e)	Unit weight (kN/m³)	PI (%)	Water content (%)	Testing device
I	1	3.52	8.57	15.1	8.4	11.760	239	273	ITC
I	2	3.52	9.18	15.1	8.4	11.860	239	268	RC
I	3	3.5	8.59	19.7	6.7	11.960	197	245	ITC
I	4	3.52	9.32	19.7	6.5	12.050	197	238	RC
II	5	3.5	8.52	19.5	6.0	11.960	183	255	ITC
II	6	3.52	8.52	25.5	6.6	12.160	101	221	ITC

Note: ITC – Instrumented Triaxial Cell.
RC – Resonant Column.

Table 2
The best-fit parameters for V_s measurement with the instrumented triaxial chamber varying the isotropic effective stresses of Specimen no. 1.

Specimen no.	Loading stage	Effective pressure (kPa)	V_s (m/s)	Excitation frequency (kHz)	wave-length, λ (m)	d/λ	A_s (m/s)	n_s	m_v, average 1/kPa	V_s estimated at mean stress (m/s)
1	1st loading	25	35.3	2.0	0.018	5	53	0.26	0.00086	46.7
		49	42.2	2.0	0.021	4				
		74	49.0	2.0	0.024	3				
		98	56.2	2.0	0.028	3				
	1st unloading	49	51.4	2.0	0.026	3	56	0.1	0.00049	51.9
		25	49.0	2.0	0.024	3				
	2nd loading	74	52.3	2.0	0.026	3	59	0.17	0.00023	55.3
		123	60.7	2.0	0.030	3				
		147	66.0	2.0	0.033	3				
	2nd unloading	98	66.0	2.0	0.033	3	65	0.02	0.00055	45.8
		49	63.2	2.0	0.032	3				
		25	63.2	2.0	0.032	3				
	3rd loading	74	63.2	2.0	0.032	3	65	0.02	0.00015	50.0
		123	66.0	2.0	0.033	3				
		172	72.3	2.0	0.036	2	67	0.22		
		196	77.8	2.0	0.039	2				

Table 3
The best-fit parameters for V_s measurement with the instrumented triaxial chamber varying the isotropic effective stresses of Specimen no. 3.

Specimen no.	Loading stage	Effective pressure (kPa)	V_s (m/s)	Excitation frequency (kHz)	wavelength, l (m)	d/l	A_s, (m/s)	n_s	m_v, average 1/kPa	V_s estimate at mean stress (m/s)
3	1st loading	20	29.9	2.0	0.015	6	41	0.19	0.00076	35.8
		39	34.1	2.0	0.017	5				
		59	36.5	2.0	0.018	5				
		78	39.3	2.0	0.020	4				
	1st unloading	39	38.8	2.0	0.019	4	40	0.06	0.00047	41.4
		20	36.1	2.0	0.018	5				
	2nd loading	59	39.7	2.0	0.020	4	43	0.12	0.00017	46.8
		98	42.4	2.0	0.021	4				
		118	45.5	2.0	0.023	4				
	2nd unloading	78	44.9	2.0	0.022	4	45	0.07	0.00056	38.2
		39	43.0	2.0	0.022	4				
		20	40.3	2.0	0.020	4				
	3rd loading	59	43.0	2.0	0.022	4	46	0.24	0.00017	43.6
		98	45.5	2.0	0.023	4				
		137	48.3	2.0	0.024	4				
		157	51.5	2.0	0.026	3				
		177	55.1	2.0	0.028	3				

Table 4
The best-fit parameters for V_s measurement with the instrumented triaxial chamber varying the isotropic effective stresses of Specimens no. 2 and 4.

Specimen no.	Loading stage	Effective pressure (kPa)	V_s (m/s)	A_s (m/s)	n_s
2	Loading	25	45.4	60	0.21
		49	51.7		
		74	57.0		
		98	60.6		
	Unloading	49	58.3	61	0.10
		25	52.6		
4	Loading	25	47.6	57	0.12
		39	50.9		
		59	53.9		
		78	56.6		
	Unloading	39	56.3	58	0.04
		20	53.3		

4.1. Variation of V_s with effective stresses

Empirical power-law expressions to model the variation of shear wave velocities (V_s) with effective stresses, σ'_o were best-fitted to the experimental data [13]:

$$V_s = A_s \left(\frac{\sigma'_o}{P_a}\right)^{n_s} \quad (1)$$

where A_s are the values of shear wave velocities at the atmospheric pressure P_a=1 atm (100 kPa); n_s is a dimensionless exponent.

For ideal arrays of ideal materials n_s in Eq. (1) is 0.25 (visco-plastic lead spheres) [14]; the same value is also displayed by low plasticity normally consolidated fine soils from the Campeche Sound in the Gulf of Mexico [15], as well as by dry, loose to medium dense, clean sands [10]. Nevertheless, n_s can vary between 0.17 and 0.48 for other soils and that it can possibly vary with soil plasticity [16].

Power laws for materials having water contents and plasticity index values as large as the ones displayed by the Texcoco Lake clay (see Table 1) have not been used previously. Typical results are given in Figs. 3 and 4, which shows V_s values measured varying effective stress, fitting power laws during successive isotropic loading–unloading cycles. The summary of results given in Tables 2 and 3 shows that A_s increases with each successive loading cycle; upon unloading, A_s varies marginally with respect to the value attained during the previous loading cycle. Regarding

n_s, its values tend to diminish with each successive loading cycle and become very small during unloading, *i.e.* shear wave velocity becomes much less sensitive to variations of effective stress when the samples become overconsolidated (Table 5).

The graphs in Fig. 5 illustrate the effect of plastic index on the values of V_s while varying the effective consolidation stresses in Specimens 1, 3, 5 and 6. As seen, A_s values fall within the 40–60 m/s range, while exponents n_s vary from 0.26 to 0.32 to normally consolidated clay. On the other hand A_s for overconsolidated clay fall within the 42–73 m/s while exponents n_s vary from 0.09 to 0.11. (see Table 6). Differences of plasticity index did not noticeably affect the result, which is consistent with findings reported by Vucetic and Dobry [17].

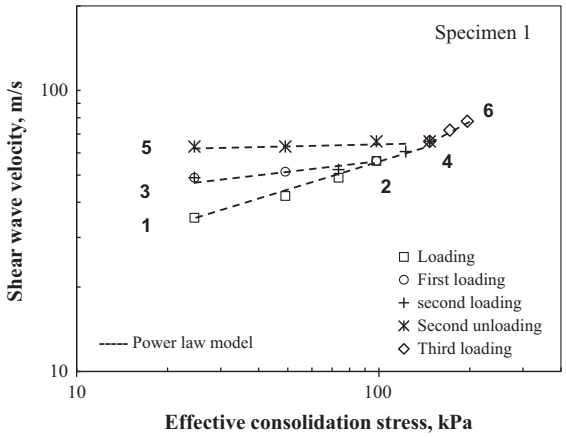

Fig. 3. Effect of loading–unloading cycles of isotropic stress on shear wave velocities in Specimen 1.

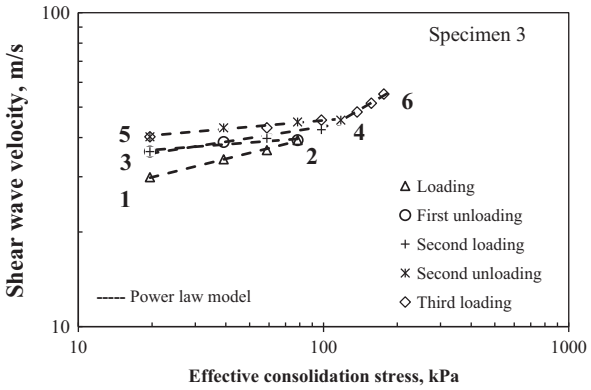

Fig. 4. Effect of loading–unloading cycles of isotropic stress on shear wave velocities in Specimen 3.

4.2. Relationship between isotropic coefficient of volume compressibility and V_s

The relationship between the isotropic coefficients of volume compressibility (m_{vi}) and shear wave velocities is studied in this section. Using the isotropic compression curves for Specimens 1 and 3. We estimated average values of m_{vi} which were then correlated to V_s calculated with the power law model at the corresponding mean stress.

Fig. 6 and data given in Tables 2 and 3 show that values of m_{vi} decrease three to four times as isotropic stresses increase during isotropic loading. Upon unloading, m_{vi} values increased about twice while shear wave velocity reduced only slightly.

4.3. Variation of the G_{max} with OCR

The small-strain shear modulus was obtained from V_s values determined from bender element measurements. The graph in

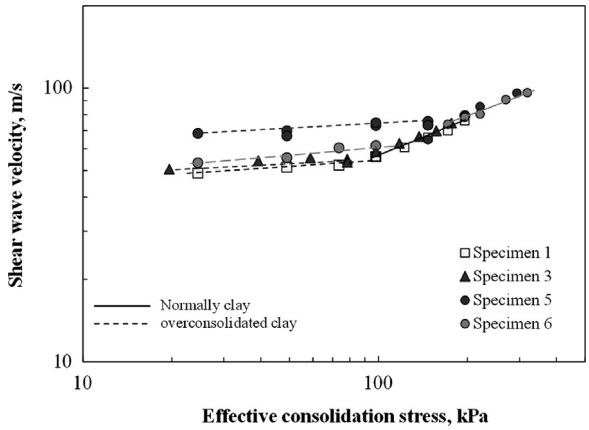

Fig. 5. Effect of plasticity on shear wave velocities of normally and overconsolidated clay.

Table 5
The best-fit parameters for V_s measurement with the instrumented triaxial chamber varying the isotropic effective stresses of Specimens no. 5 and 6.

Specimen no.	Loading stage	effective pressure (kPa)	V_s (m/s)	Excitation frequency (kHz)	wavelength l (m)	d/l	A_s (m/s)	n_s	m_v, average 1/kPa	V_s estimate at mean stress (m/s)
5	1st loading	147	64.80	2.0	0.032	3	63	0.28	0.00057	81
		196	79.38	2.0	0.040	2				
		221	85.58	2.0	0.043	2				
		294	95.92	2.0	0.048	2				
	1st unloading	147	75.60	2.0	0.038	2	73	0.07	0.005	72
		98	72.99	2.0	0.036	2				
		49	69.78	2.0	0.035	2				
		25	68.28	2.0	0.034	2				
6	1st loading	172	73.84	2.0	0.037	2	60	0.33	0.00052	84
		196	78.40	2.0	0.039	2				
		221	80.38	2.0	0.040	2				
		270	90.71	2.0	0.045	2				
		319	96.21	2.0	0.048	2				
	1st unloading	98	61.65	2.0	0.031	3	62	0.11	0.002	57
		49	55.70	2.0	0.028	3				
		25	53.36	2.0	0.027	3				

Fig. 7 shows values of G_{max} divided by the effective stress and plotted against the overconsolidation ratio (OCR) obtained with the instrumented triaxial cell. As seen there, stress-adjusted G_{max} increases as OCR increases. This finding is consistent with results presented elsewhere [17]. The mean increment of stress-adjusted G_{max} is about 300% when OCR increases from 1 to 4 considering all the specimens.

4.4. Resonant column results

Specimens 2 and 4 were tested in the resonant column device and were saturated and then consolidated isotropically following the same procedures and consolidation paths as in the samples tested in the triaxial cell, applying only one isotropic loading–unloading cycle. Undrained torsional loading that lasted about 2 h was applied after each increment or decrement of isotropic stress and then consolidating the specimens for 24 h.

The graphs in Fig. 8 show the relationships between V_s and effective stress for the loading–unloading stage in RC tests, for Specimens 2 and 4. Results are summarized in Table 4 and are qualitatively similar to those obtained from bender element determinations performed in the triaxial cell. Data presented there show that the reference shear wave velocity, A_s, is affected only marginally during unloading. In the loading branch n_s values are smaller than those obtained for the specimens tested in the triaxial cell and are rather low during the unloading branch, a result of overconsolidation.

5. Comparisons between laboratory and field results

In this section we compare shear wave velocities measured in the laboratory (resonant column and triaxial cell with piezoelectric crystals) with V_s values measured in the field with a seismic cone that was performed only 5 m away from the borehole used to retrieve the soil samples used in this research. Horizontal impacts on wood or metal planks at the ground surface generate SH waves that propagate downwards and are received by geophones placed near the conical tip. Details of the techniques used in seismic cone testing have been published elsewhere [18]. The geophones in the seismic cone operate in the 2–4600 Hz frequency range; their natural frequency is 2 Hz.

Data in Fig. 9 show the shear wave velocities measured with the three different experimental techniques. In selecting V_s values from the bender element measurements and from the resonant column tests it was assumed that the soil is slightly overconsolidated *in situ i.e.* those values were obtained from the unloading–reloading fits of Figs. 3 and 4. As shown, V_s measured with the seismic cone, the resonant column and bender elements at a depth of 15.1 m was 45, 51 and 55 m/s, respectively and at 19.7 m of depth, 54, 52 and 45 m/s, respectively. Estimated effective stresses applied to the specimens tested in laboratory were 35 and 45 kPa corresponding to 15.1 and 19.7 m of depth, respectively.

Shear wave velocities measured with the seismic cone and with the resonant column differ by only a small amount. Those measured in soil specimens in the instrumented triaxial cell with bender elements and with the resonant column exhibit evident differences but the overall scatter of V_s values is not large 7% and 15% at 15.1 and 19.7 m deep.

Differences may only marginally be attributed to variations in the initial index properties of the samples (varying 3% and 2% in water contents and void ratio respectively). More importantly, discrepancies in V_s values can be attributed to the differences in stress and strain paths during torsional loading in the resonant column and in bender element measurements. On the other hand,

Table 6
Effect of plasticity on shear wave velocities of normally and overconsolidated clay.

Specimen no.	Normally consolidated clays			Overconsolidated clay		
	PI	A_s	n_s	PI	A_s	n_s
1	239	53	0.26	239	56	0.10
3	197	40	0.3	197	42	0.07
5	183	63	0.28	183	73	0.07
6	101	60	0.33	101	62	0.11
Overall general expression		54	0.29		58	0.09

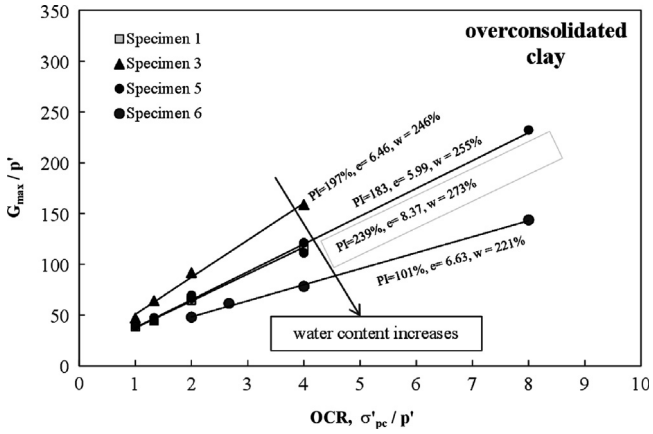

Fig. 7. Variation of the stress-adjusted G_{max} with OCR.

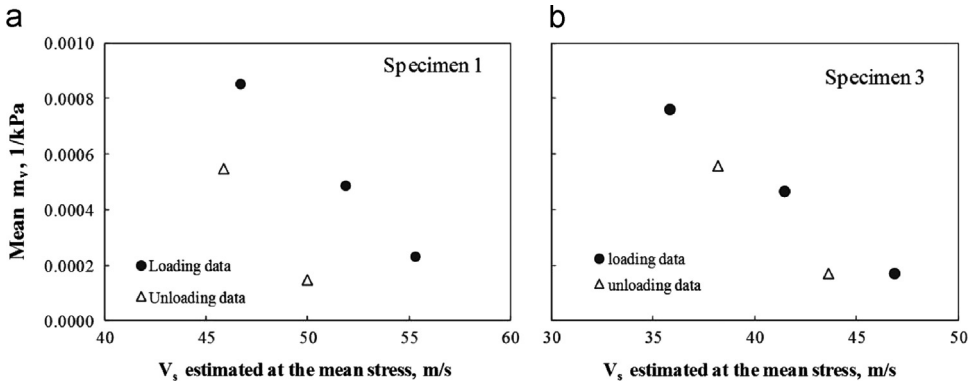

Fig. 6. Mean m_{vi} varying with the estimated V_s at the mean stress of each loading–unloading cycle. Part (a) Specimen 1 and part (b) Specimen 3.

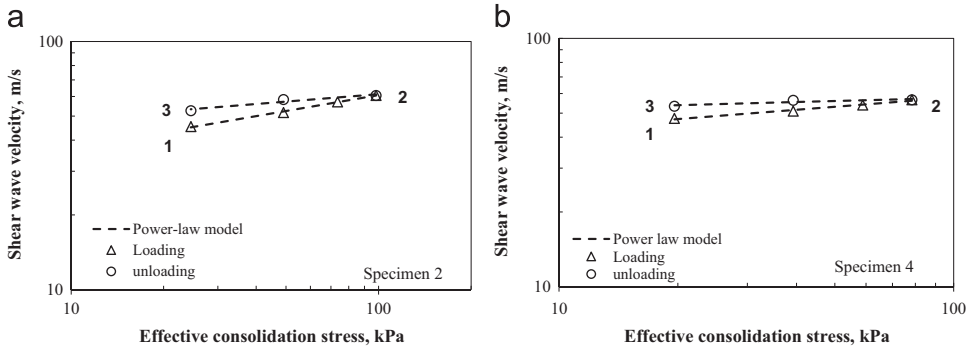

Fig. 8. Shear wave velocities from resonant column tests applying one isotropic loading–unloading cycle. Part (a) Specimen 2 and part (b) Specimen 4.

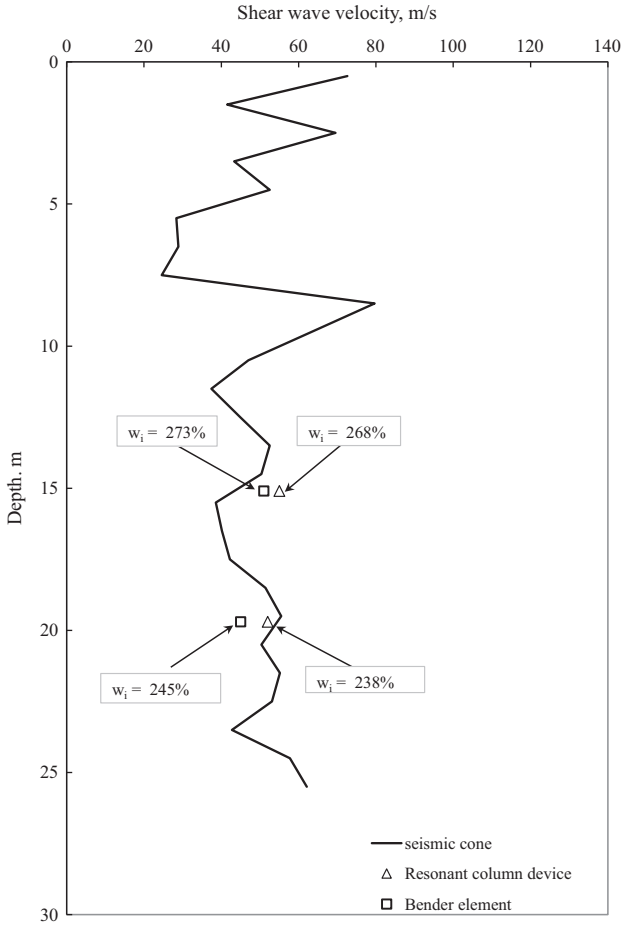

Fig. 9. Shear wave velocities determined *in situ* with the seismic cone and in the laboratory with bender elements and from resonant column tests.

strain levels are also very different in each of the experimental techniques as well as the excitation frequencies which are also significantly different in the three experimental techniques discussed here. Mechanical disturbance during sampling and in the laboratory will also influence the results.

Apart from the above, it should be noted that V_s measured in the field may be affected by the way in which field data are processed, especially if these velocities are actually average values of the propagated waves passing through successions of soft and rigid soil strata. These structural features or others like fissures or discontinuities (large to medium scale) may not be adequately represented in element testing in the lab.

6. Conclusions

The use of piezoelectric transducers to measure S wave velocities in soils from the former Texcoco Lake, north of Mexico City, is a novelty.

Power laws had never been used previously to obtain relationships between V_s and effective stress along loading–unloading cycles of isotropic stress applied to specimens in the instrumented triaxial cell and in a resonant column device, in materials having water contents and plasticity index values as large as the ones displayed by the Texcoco Lake clay.

Experimental results showed that there exist different relationships between the isotropic mean coefficients of volume compressibility (m_{vi}) and V_s, depending on the stress state and the stress history, *i.e.* depending on whether the specimen state lied on the virgin consolidation line or on a loading–reloading branch.

Our results also showed that V_s measured with bender elements are not affected by plasticity for soil samples in normally consolidated state, for the range of plasticity indices of the specimens tested in our investigation. Stress-adjusted, small-strain shear modulus increases as OCR increases: G_{max}/p' shows an increment of about 300% when OCR goes from 1 to 4.

Additionally we compared V_s values determined from field seismic cone tests with those obtained in the lab with bender elements and in a resonant column device. V_s values obtained from each experimental technique turned out to be different. These differences can be attributed to several factors, all of which must be the object of future studies. Finally, no matter what the cause or causes of the discrepancies in the V_s values determined with the resonant column, the bender elements or the seismic cone, the key point is that the maximum difference in all these values is in the 7–15% range.

Acknowledgments

The authors deeply appreciate Dr. M. Tanaka from the Port and Airport Research Institute, Japan, for his permission to include and use the field testing information from the Texcoco Lake site.

References

[1] Marsal R, Mazari M. The subsoil of Mexico City. Mexico City: Facultad de Ingeniería, UNAM; 1959.
[2] Carrillo N. The subsidence of Mexico City and Texcoco Lake, Texcoco project; 1969.
[3] Ovando E, Ossa A, Romo MP. The sinking of Mexico City: its effect on soil properties and seismic response. Int J Soil Dyn Earthq Eng 2007;27:333–43.
[4] Romo MP, Jaime A, Reséndiz D. General soil conditions and clay properties in the Valley of Mexico. J Earthq Spectra 1988;4(2):731–52.

[5] Romo MP Ovando E. Modelling the dynamic behaviour of Mexican clays. In: Proceedings of the 11th world conference on earthquake engineering. Acapulco, Mexico; 1996.
[6] Mayoral JM, Romo MP, Osorio L. Seismic parameters characterization at Texcoco lake, Mexico. Soil Dyn Earthq Eng 2008;28:507–21.
[7] Romo MP, Auvinet G, Ovando E, Mendoza MJ, Taboada VM, Lermo JY, Mooser F. Ingeniería Geotecnia para el nuevo aeropuerto internacional de la Ciudad de México: soluciones en el exLago de Texcoco y en Zapotlán de Juárez, Informe del Instituto de Ingeniería, UNAM, a Aeropuertos y servicios Auxiliares; 2001.
[8] Fam MA, Santamarina JC. Study of geoprocesses with complementary mechanical and electromagnetic wave measurements in an oedometer. Geotechn Test J 1995;18(3):307–14, http://dx.doi.org/10.1520/GTJ10999J.
[9] Viggiani G, Atkinson JH. Interpretatión of bender elements tests. Géotechnique 1995;45(1):149–54.
[10] Valle-Molina C, Stokoe KH. Seismic measurements in sand specimens varying degrees of saturation using piezoelectric transducers. Can Geotechn J 2012;49 (6):671–85.
[11] Skempton AW. The pore-pressure coefficients A and B. Geotechnique 1954;4 (4):143–7.
[12] Santoyo E. Exploración de suelos: métodos directos e indirectos, muestreo y pruebas de campo. In: Vigésima conferencia Nabor Carrillo, XXV Reunión Nacional de la Sociedad Mexicana de Ingeniería Geotécnica, Acapulco, Mexico; 2010.
[13] Hardin BO. The nature of stress–strain behavior of soils. In: Proceedings of geotechnical engineering division specialty conference on earthquake engineering and soil dynamics, vol. 1, ASCE. Pasadena, June; 1978. p. 3–90.
[14] Cascante G, Santamarina JC. Interparticle contact behaviour and wave propagation. ASCE J Geotech Eng 1996;122(10):831–9.
[15] Valle C, Stokoe KH. Laboratory measurements of the dynamic properties of intact and remolded offshore clays from Campeche Bay. In: Proceedings of offshore mechanics and Artic engineering conference, OMAE´2003, American Society of Mechanical Engineers, paper No. 37248, workshop of offshore geotechnics, Cancun, Mexico, June; 2003.
[16] Fam M, Santamarina JC. A study of consolidation using mechanical and electromagnetic waves. Geotechnique 1997;47(2):203–19.
[17] Vucetic M, Dobry R. Effect of soil plasticity on cyclic response. J Soil Geotechn Eng Div, ASCE 1991;117(1):89–107.
[18] Robertson PK, Campanella RG, Members ASCE, Gillespie D, Rice A. Seismic CPT to measure in situ shear wave velocity. J Geotech Eng 1986;112(8):791–803.